Single Mode Fiber Array for Planet Detection using a Visible Nulling Interferometer

Duncan Liu, B. Martin Levine, Michael Shao, and Franciso Aguayo
Jet Propulsion Laboratory, California Institute of Technology
4800 Oak Grove Drive
Pasadena, CA 91109
818-354-9508, duncan.liu@jpl.nasa.com, 818-393-6669, bruce.m.levine@jpl.nasa.gov, 818-354-7834, Michael.shao@jpl.nasa.gov, 818-393-7384, Francisco.aguayo@jpl.nasa.gov

Abstract— We[1] report the design, fabrication, and testing of a coherent large mode field diameter fiber array to be used as a spatial filter in a planet finding visible nulling interferometer. The array is a key component of a space instrument for visible-light detection and spectroscopy of Earth like extrasolar planets. In this concept, a nulling interferometer is synthesized from a pupil image of a single aperture which is then spatially filtered by a coherent array of single mode fibers to suppress the residual scattered star light. The use of the fiber array preserves spatial information between the star and planet. The fiber array uses a custom commercial large mode field or low NA step-index single mode fiber to relax alignment tolerances. A matching custom micro lens array is used to couple light into the fibers, and to recollimate the light out of the fiber array. The use of large mode field diameter fiber makes the fabrication of a large spatial filter array with 300 to 1000 elements feasible.

TABLE OF CONTENTS

1. INTRODUCTION

A planet detection method that uses a single-mode spatial filter array following a visible nulling interferometer has been proposed, and a laboratory demonstration is currently being investigated [1-4] . The detection of a planet next to the parent star in visible light spectrum requires a 10 billion to 1 contrast ratio using the conventional coronagraph imaging system. This requirement leads to extremely tight fabrication tolerances. The proposed spatial filter-based nulling interferometer reduces this contrast ratio requirement to 10 million to 1, which is an improvement of 3 orders of magnitude.

In the nulling interferometer approach, the star and planet beams at the pupil of the telescope are splitted, sheared, one beam phase shifted by π with respect to the other beam, and recombined to cancel the on-axis star beam as illustrated in Figure 1. The off axis planet light if located just far enough so that the π phase shift is compensated, constructive interference will take place and show up in the imaging plane. However, as in conventional coronagraph, the 10 billion to 1 contrast ratio between parent star and planet will impose extremely tight tolerance on the interferometer optics. Mainly, the optics in the two arms of the interferometer needs to be extremely symmetrical across the beam so that the two beam when combined have matched spatial pattern.

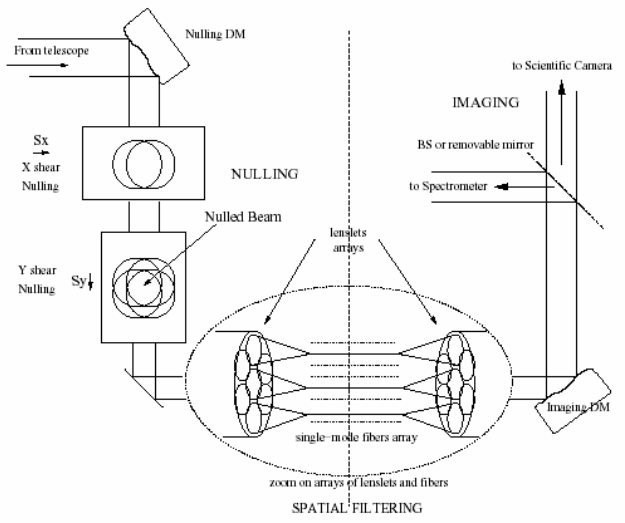

Figure 1 Schematics of a planet detection optical system using nulling interferometer and spatial filtering. (From Ref [1])

[1] 0-7803-8155-6/04/$17.00©2004 IEEE

It has been shown that a single-mode spatial filter such as a single mode fiber can be used at the beam combiner output to shape the combined beams to have a single spatial pattern or mode. This is because a single mode fiber only guides a single fundamental mode and leaks out higher-order modes. In principle, if a single mode fiber can suppress the higher-order modes by -30 dB to -40 dB over the fundamental mode, one can reduce the contrast ratio requirement of the nulling interferometer by 3 orders of magnitude.

A single mode fiber erases the spatial information of the incident beam. To preserve the spatial information or wavefront of the incident beam at the pupil, a two dimensional single-mode fiber array and spatially matched lens arrays are needed. In principle, to detect a Jupiter-like planet from the parent star at 10pc, 300 pixels or fibers are needed. For earth-like planet, 1000 pixels are needed.

The useful visible-to-near-infrared spectral range to planet science is from 500nm to 1100nm. A typical commercial single mode fiber is designed to have an NA approximately >0.1 near 2nd-order mode cutoff wavelength of the fiber so that bending loss is negligible under normal condition in most applications. This leads to a mode-field-diameter (MFD) of approximately 3.5 μm near the cutoff wavelength. Put this number together with the +/- 2 μm fiber center-to-center spacing tolerance of a typical 10x10 commercially available fiber array, it would not be very predictable if one can align lens array to a fiber array with 300 to 1000 elements.

Previously we built a fiber array with 120 fibers using a commercial, ~0.1NA, Mode-Field Diameter (MFD) 0.35 μm, single-mode fiber. The 10% alignment sensitivity, i.e. fiber offset needed for a 10% coupling efficiency drop, for this fiber is ~0.6 μm. To alleviate the high alignment sensitivity associated with conventional single mode fiber, we also demonstrated a small NA (~0.04), large MFD (12 μm) Photonics Crystal Fiber (PCF) array. The 10% alignment sensitivity of this fiber is ~ 2 μm. However, the preparation of a PCF array is fairly complicated and expensive and PCF has a fiber coupling bandwidth slightly narrower than a conventional single mode fiber.

In this paper, we present the fabrication of a fiber array made with a custom small NA (~0.04) conventional single mode fiber to alleviate the problem associated with regular 0.1NA fiber array and 0.04 PCF array.

2. FIBER ARRAY AND LENS ARRAY

The single-mode spatial filter array consists of a two dimensional single mode fiber array sandwiched by two matching micro-lens array as shown in Figure 2 with only 4 elements in the array for illustration purpose.

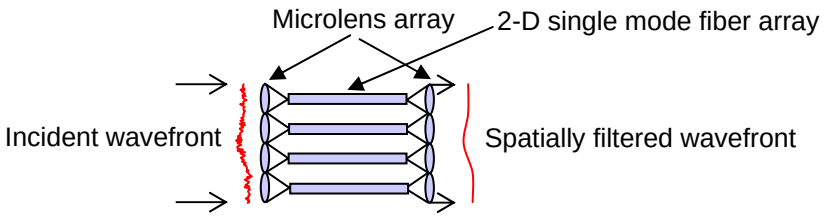

Figure 2 A single mode spatial filter array consists of an input lens array that divides incident wavefront into multiple segments and couple light in each segment into a single mode fiber, which removes higher-order spatial modes from each light segment; a second lens array recollimates the light from each fiber.

The quality of the incident wavefront needs to be preserved at the 1/10 wave rms level across the array. This means two ends of the fiber array need to be polished to 1/10 wave rms and parallel with each other to 1/10 wave across the array. The fibers need to be perpendicular to the end faces of the fiber array to the same degree as the parallelism between the two end faces. In theory if the higher-order modes will be absorbed completely as they leak to the cladding surface, the minimum length of the fiber array is less than a few centimeters. Practically, the length of the fiber array needs to be longer to allow a slower absorption/scattering of leaked higher-order modes. To maximize the filling factor (or throughput), the array geometry of the lens and fiber arrays is a 2 dimensional closely packed hexagonal structure.

Fiber Array

The design of the fiber array is based on the use of 3 precision equilateral prisms placed on a flat base plate as shown in Figure 3. The middle prism has one of its vertices polished flat to a width approximately equal to the side length of the fiber array to be built. The fiber array is confined by two facing sides of the upright prisms and the flat top of the middle prism. The width of the flat top of the middle prism is polished to be approximately one fiber diameter less than the side length of the fiber array to ensure the middle prism touches and confines the fiber array from the top. For a maximum 10% efficiency drop or a 2 μm offset, the maximum angular offset of a 1027 hexagonal fiber array in a 1540 triangular array using 300 μm cladding

diameter fiber, is ~ 20 arc seconds. This is the tolerance specification for the vertex angle of the equilateral prisms. The bottoms of the prisms when placed on the base flat also need to be parallel with each other by 20 arc seconds. This is can be controlled by observing the interference fringes generated between the prism base and the base flat. We used a prism with a height of 15 mm. The maximum number of fringes in visible wavelength is approximately 3.

When the longer sides of the prisms are not parallel with each other, the fiber array will see a triangle formed by the

The outer geometry tolerance discussed above controls the systematic error. However, it does not control the random error caused by the concentricity of fiber core and cladding and the fiber cladding diameter to a less degree. For the standard 125 μm and custom 300 μm cladding fibers, the concentricity tolerances are 0.5 and 1.5 μm, respectively. The cladding diameter can be very uniform if the fiber segments are cut from the same section of a fiber lot. Thus the larger the cladding diameter the larger the random error will be in the fiber spacing. In general, the spacing variation can be on the order of 3 μm for the 300 μm cladding fiber.

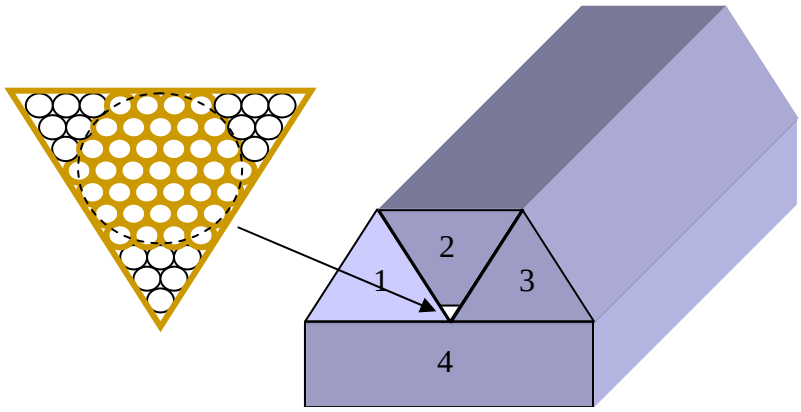

Figure 3 Fiber array is made by confining fibers with equilateral prisms 1 and 2 and equilateral prism 2 with one vertex polished off to have a width given by that of the fiber array plus the diameter of one fiber.

3 prisms deviated from being equilateral. If we impose the same 20 arc second tolerance requirement on this triangle, it can be calculated that the longer sides of the prisms need to be parallel with each other within 2.42 degrees. However, another restriction is that the gap created by this needs to be less than the diameter of the fiber, otherwise the bottom fiber will slip through the gap. For example, for a fiber with a cladding diameter of 300 μm and a prism length of 72cm, the maximum angle between the two long sides of the prisms is 1.43 arc minutes, which is much smaller than the 2.42 degree tolerance mentioned above. However, in order to use the prism for measuring the perpendicularity between the fiber and its end faces the fiber needs to be perpendicular to the end face of the prism within 20 arc seconds. This requires the two long sides of the prism to be parallel within 22 arc seconds. For a 72cm long prism, this means the gap between the two prisms at the base needs to be < 80 μm. As a result, the criteria for determining if the two prisms are placed parallel enough can be to visually make sure the gap between the bases of the two prisms be smaller than ¼ of the fiber diameter on two ends of the prism assembly. In order to use the prism as the reference for controlling the perpendicularity of the fiber end face the prism also needs to be the reference when the two ends of the fiber array are polished.

This will cause the coupling efficiency to drop 30% from the peak value.

Micro-Lens Array

Commercial micro-lens array such as epoxy molded and gray-scale photolithography etched fused silica lens arrays are being used in this work. In general, the former has a center to center spacing tolerance of 1 to 2 μm, while the latter of 0.5 μm.

The spacing accuracy of the gray-scale photolithography etched micro-lens array is 4 to 6 times higher than that of a fiber array. It is then possible to measure the absolute fiber spacing and use it to design and fabricate the matched lens array. This can reduce the systematic alignment error between the lens array and fiber array. If the individual fiber positions can be measured, in principle, a lens array can be fabricated with matched positions. This can then also reduce the random error from approximately 3 μm to 1 μm and can potentially reduce the coupling efficiency variation from 30% to < 10%.

If the lens is designed on the side facing fiber array, the distance between the lens array and the fiber array can be controlled by a precision spacer. If the lens is designed on the side of the substrate opposite to the side facing the fiber array, the distance between the lens array and fiber array is

controlled by the thickness of the substrate or a substrate plus a precision spacer. The former is used in with the epoxy molded lens array and the latter is used in with the gray-scale photolithography etched lens array. The advantage of the latter is index matching epoxy can be used to bond the lens array and fiber array and this in turn reduces the wavefront distortion that can be caused by the irregular surface on the fiber array.

3. ALIGNMENT AND ASSEMBLY

Once the fiber array is fabricated the lens array needs to be aligned and bonded to the fiber array on two ends. The alignment techniques are different for the first and the second lens array.

Figure 4 depicts the the alignment system. The detailed alignment procedure are described in Ref [5]. The alignment system basically consists of a Zygo interferometer, which is used for aligning the fiber array and the lens array to be parallel with each other, and a 6 axis stage with 0.2 μm alignment resolution, which is used for lens and fiber array alignment. We describe the alignment and assembly procedures for the first lens array and the second lens array, respectively, as follows,

Alignment of First Lens Array to Fiber Array

A flat mirror is first attached to one end of the fiber array. The mirror reflects the light back into the Zygo to generate a fringe pattern, which is in turn used to check the focus of each lenslet in the lens array. Once the fiber array and lens array are aligned by rotating and translating with respect to each other they are bonded according to the method described in Ref [5].

Alignment of Second Lens Array to Fiber Array

The mirror can not be directly attached to the first lens array on the fiber array now because by the lens is designed to making contact with air or vacuum. To align the second lens array, a mirror is first aligned to be perpendicular to the Zygo output wavefront. Then the fiber array is placed with the first lens array facing the mirror and the front surface of the fiber array is aligned to be parallel with the Zygo output wavefront and thus with the mirror. Then the second lens array is aligned to be parallel with the Zygo output wavefront and thus with the fiber array and mirror. Then the same alignment procedures in aligning and bonding first lens array to the fiber array are used to align the second lens array.

4. MAPPING OF FIBER POSITIONS

Using a variation of our alignment set up, and using the interferometer as a light source, we can simultaneously measure the placement accuracy of all fibers in the array.

As shown in Figure 5, a lens array on the alignment fixture is positioned to couple its focused light (and not necessarily be optimal alignment) into each of the fibers. A CCD camera with a 50mm diameter magnifying image relay system records the spot pattern. The focal length, f_1 and f_2 of the imaging system are 20cm and 30 cm, respectively. The CCD camera has 1392 x 1040 pixels with 6.4 μm square pixels. An aperture stop is placed at the pupil plane to control the f/number of the optical system. Changing the f/number controls the spot size and the number of pixels per spot on the CCD camera. The aperture diameter control range is from ~1mm to ~50 mm using discrete stops. For a 19 mm diameter stop, the FWHM width of the spot is about 3 to 4 pixels.

A measure of array regularity is calculated by the rms difference between these measured centroid positions and the theoretical positions of a regular array with constant spacing (see Figure 6). The regular array is made by an e-beam photolithography machine. The placement accuracy is much less than 0.1 μm or two orders of magnitude better than that of the fiber array

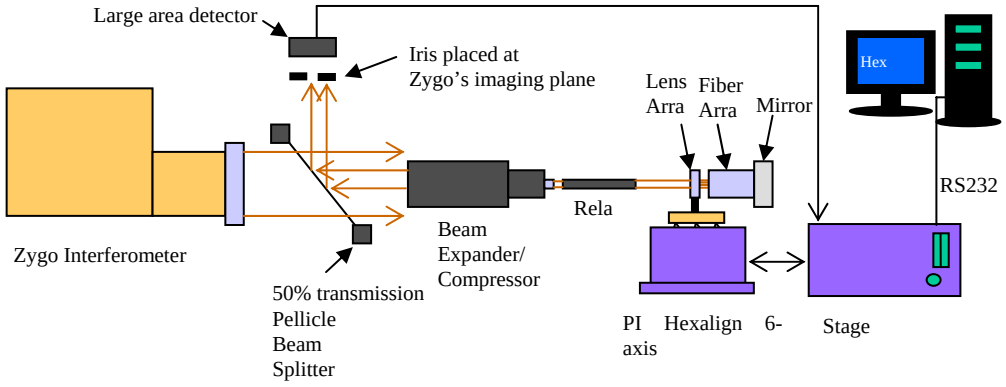

Figure 4 Schematic diagram for lens array to fiber array alignment system.

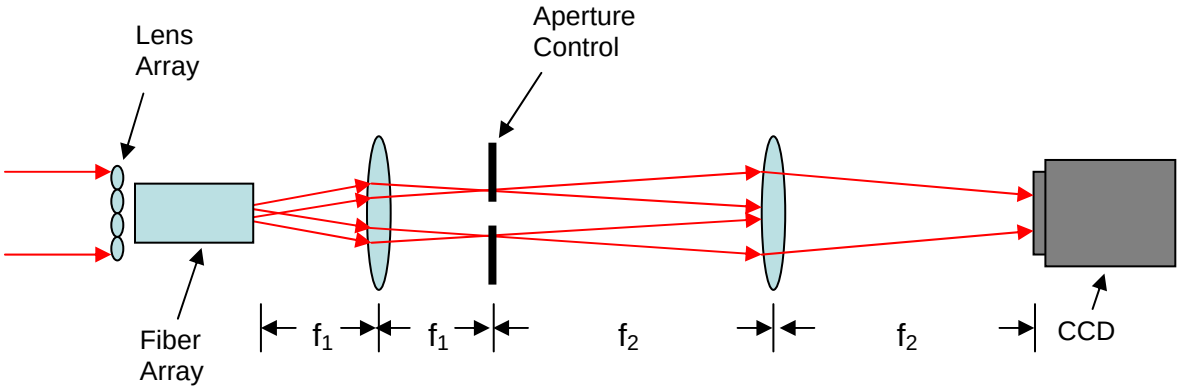

Figure 5 Setup for fiber position mapping using centroid method

5. EXPERIMENTAL RESULTS

We have built a 120/41 (triangle/hexagon) fiber array using 3.5 μm MFD single mode fiber (see Figure 7) and a 496/331 (triangle/hexagon) fiber array (see Figure 9) using a custom 8.5 μm MFD single mode fiber at 500 nm wavelength. The cladding of the fiber is 126 μm nominally. The spacing uniformity of these fiber arrays is much better than that of the fiber arrays reported in Ref [5] due to an improvement in the fiber laying process.

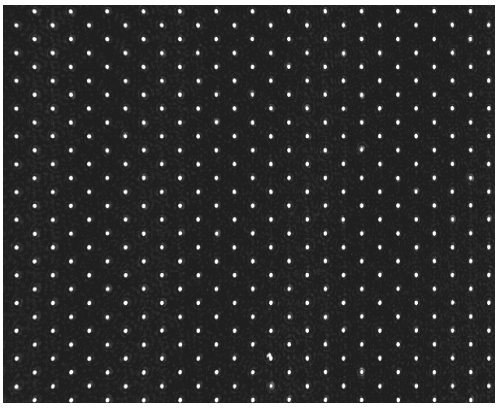

Figure 6 Reference mask made with e-beam photolithography with constant spacing.

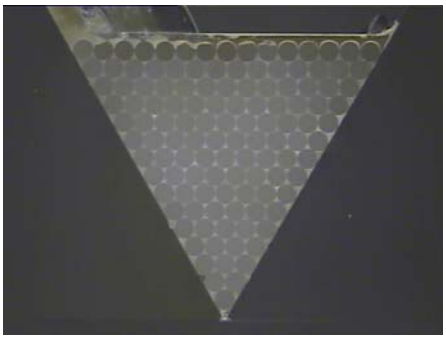

Figure 7 Polished end of the small core 120/41 (triangle/hexagon) fiber array.

Figures 8 and 10 show the light output of the two fiber arrays when a collimated HeNe laser beam is coupled into the fiber array via a lens array. The large core 496/221 fiber array is clearly better than the small core 120/41 fiber array in both the uniformity and percentage of fibers that have light coupled into them. It is also worth noting that the better coupled 496/221 fiber array has 4 times more fibers than the 120/41 fiber array.

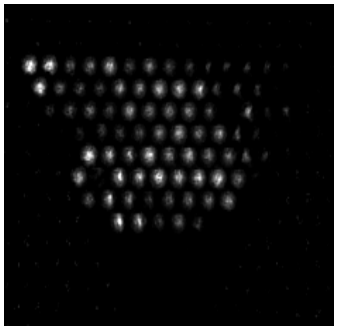

Figure 8 Light output of the small core 120/41 (triangle/hexagon) fiber array. A HeNe laser beam is coupled into the fiber array via a lens array.

Comparing Figures 8 and 10 clearly demonstrates that the use of a large mode field diameter fiber can greatly relax the alignment sensitivity of a large, two-dimensional, single-mode lens-fiber array.

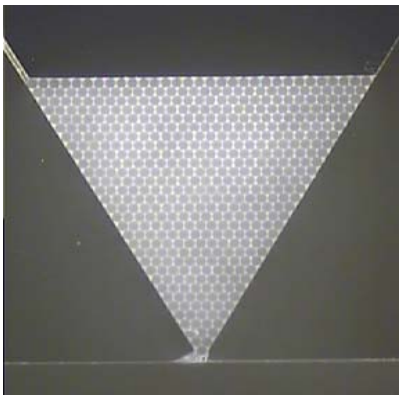

Figure 9 Polished end of the large core 496/331 (triangle/hexagon) fiber array.

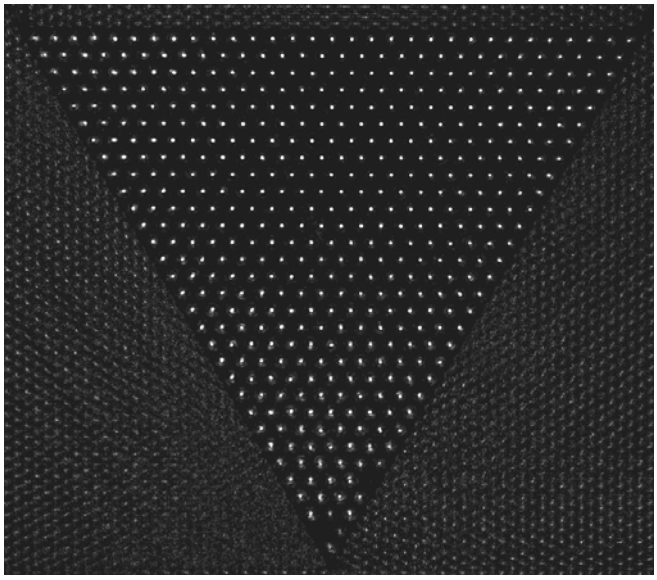

Figure 10 Light output of the large core 496/331 fiber array when light is coupled into the array via a lens array. The output end does not have a lens array. The detailed uniformity of the spot intensity is not revealed by this photo due to increased brightness and contrast adjustment over the original photo for the purpose of clarity.

6. FUTURE WORKS

We plan to align and bond the lens array to the large core fiber array reported in this paper and characterize the wavefront distortion caused by this array. In addition, we plan to build another 496/331 (triangle/hexagon) fiber array using a 300 μm cladding diameter and 12 μm mode field diameter single mode fiber with a cutoff wavelength of 500 nm. The 300 μm cladding diameter is chosen to match half of the spacing of the deformable mirror to be used in a future system demonstration.

Limited by the fabrication capability as the cladding diameter increases the concentricity of the fiber core can decrease. For the 125 μm cladding fiber used in this work, the concentricity of the fiber core and cladding is 0.5 μm, while for the 300 mm one, it is 1.5 μm according to the manufacturer's specification. To reduce the impact of this increase, we also plan to map the individual fiber position and explore the feasibility of fabricating a custom lens array with matched positions to improve the uniformity of coupling efficiency.

7. SUMMARY AND CONCLUSIONS

We have demonstrated the feasibility of fabricating a single mode fiber array with 496 fibers in a triangle or 331 fibers in a hexagon confined by 3 precision prisms with light coupled across the entire fiber array. This is feasible with the use of a custom large mode field diameter fiber, which greatly relaxes the lens array to fiber array alignment sensitivity. The fiber array is design and built for performing spatial filtering in high-contrast planet detection using nulling interferometer, which reduces imaging contrast requirement by 3 orders of magnitude. The 496/331 (triangle/hexagon) fiber array can enable detection of Jupiter-like extrasolar planets in nearby stars (10pc away). The tolerance analysis shows it is possible to build a 1540/1027 (triangle/hexagon) lens-fiber array with 15% fiber coupling efficiency variation. This will make it possible to detect extrasolar earth-like planets in nearby stars.

ACKNOWLEDGEMENT

The research described in this paper was carried out at the Jet Propulsion Laboratory, California Institute of Technology, under a contract with the National Aeronautics and Space Administration.

REFERENCES

[1] Bertrand Mennesson, Mike Shao, Bruce M. Levine, James K. Wallace, Duncan T. Liu, Eugene Serabyn, C. Unwin and Charles A. Beichman, "Optical Planet Discoverer: How to turn a 1.5 m Telescope into a Powerful Exo-planetary Systems Imager," Proc. SPIE Vol. 4860, P. 32-44, 2002.

[2] B.M. Levine, Michael Shao, C.A. Beichman, B. Mennesson, R. Morgan, G. Orton, E. Serabyn, S. Unwin, and T. Velusamy, 'A Visible Light Terrestrial Planet Finder --Planet Detection and Spectroscopy by Nulling Interferometry with a Single Aperture Telescope', Proc. SPIE Vol 4852, 2002.

[3] B. Martin Levine, Michael Shao, Duncan Liu, J. Kent Wallace, and Benjamin Lane, 'Planet Detection in Visible Light with a Single Aperture Telescope and Nulling Coronagraph', Proc. SPIE Vol 5170, 2003.

[4] Michael Shao, B. Martin Levine, J. Kent Wallace, Eugene Serabyn, Duncan T. Liu, and Benjamin F. Lane, 'The Visible Nulling Coronagraph--Progress Towards Mission and Technology Development', 203rd Meeting of the American Astronomical Society, 5 January 2004.

[5] Duncan Liu, B. Martin Levine, Michael Shao, "Design and fabrication of a coherent array of single-mode optical fibers for the nulling coronagraph", Proc. SPIE Vol 5170, 2003.

BIOGRAPHY

Duncan Liu earned a BS degree in Physics in 1978 from National Cheng- Kung University in Taiwan, ROC, an MS degree in Physics in 1984 from Wayne State University, and a PhD degree in Electrical Engineering in 1987 from The Pennsylvania State University. He has worked in the fields of nonlinear optical image processing using III-V semiconductor photorefractive materials, fiber networking components, radiation effects on fiber, and photonics packaging at Jet Propulsion Laboratory from 1987 to 2000 and from 2002 to present. He was the Director of Optical Packaging for a telecom component startup company from 2000 to 2002. He is currently a Senior Member Technical Staff at the Jet Propulsion Laboratory.

B. Martin Levine earned his BS degree in 1972 from the Rochester Institute of Technology, a Masters Degree n Statistics from the Colorado State University in 1976, and a PhD in Optics from the University of Rochester in 1986. He has 20 years experience in the design and construction of adaptive optics systems working as a consultant for the US Air Force and also at Adaptive Optics Associates. Currently Dr. Levine holds the positions of Deputy Leader, Interferometry Center of Excellence, and also is the Manager of the Advance Telescopes Technologies and Concepts Office at the Jet Propulsion Laboratory, where he is working on developing advanced concepts for future space missions.

Michael Shao earned a BS in Physics in 1971, and a PhD in Astronomy in 1978, both from the Massachusetts institute of Technology. His entire professional career has been devoted toward the development and practice of astronomical observations using spatial interferometery working at the US Naval Observatory, and at the Harvard-Smithsonian Astrophysical Observatory before coming to work for JPL

in 1989. He is the Project Scientist for the Space Interferometry Mission, and the Keck Interferometer at the Jet Propulsion Laboratory, and the Director of the Interferometery Center of Excellence.

Francisco Aguayo is a junior student of The California State University at Los Angeles with a Mechanical Engineering Major. He joined JPL as a summer student in 2002 and then became a part-time employee working on the optical fiber array fabrication and testing for the visible nulling interferometer development effort at JPL.